J Porous Mater (2006) 13: 141–146
DOI 10.1007/s10934-006-7017-6

Pore structures of multi-walled carbon nanotubes activated by air, CO_2 and KOH

Yong Chen · Chang Liu · Feng Li · Hui-Ming Cheng

Received: July 11, 2005 / Revised: September 27, 2005

Abstract Multi-walled carbon nanotubes (MWNTs) synthesized by the catalytic decomposition of benzene were activated by KOH, CO_2 or air. The adsorption isotherms of the activated MWNTs were analyzed and their pore size distributions were obtained. The results showed that the specific surface areas of the MWNTs activated by KOH, CO_2 and air were increased to 785 m^2/g, 429 m^2/g and 270 m^2/g, respectively. The MWNTs activated by KOH were rich in micropores and mesopores, especially high mesopores having volumes up to 1.04 cm^3/g. The CO_2-activated MWNTs also had many micropores while the air-activated MWNTs had a much smaller micropore volume. The morphologies of the activated MWNTs were examined by transmission electron microscopy and high resolution transmission electron microscopy, and the activation mechanisms were discussed.

Keywords Carbon nanotubes · Adsorption · Electron microscopy · Pore size distributions

1. Introduction

Carbon nanotubes (CNTs) have attracted a wide research interest since they were discovered by Iijima in 1991 [1]. They are expected to have potential applications as composite reinforcement [2, 3], catalyst support [4, 5], field emitters [6], supercapacitor electrodes [7, 8], gas absorbent [9, 10], etc., because of their special characteristics, such as one-dimensional nano-scale hollow cores, high surface areas, excellent mechanical properties, and good chemical stability. In particular, a high specific surface area, sufficient pores and a suitable pore structure are highly demanded for such applications as gas adsorption and supercapacitor electrode. The theoretical specific surface area of CNTs can be very high, 2630 m^2/g for single-walled carbon nanutubes (SWNTs) with open ends [11]. However, the as-prepared CNTs are usually entangled with one another and have closed caps, so their specific surface area is quite low ($\sim 100\ m^2/g$) compared to the theoretical predictions. Some efforts, such as cutting [12], cap-opening [13, 14], or using chemical treatments to create micropores on the walls of the multi-walled carbon nanotubes (MWNTs), have been made to increase the specific surface area of CNTs. One way is to directly prepare isolated SWNTs, double-walled carbon nanotubes (DWNTs) or MWNTs with small diameter, thus increasing their external specific surface area. For example, Bacsa et al. [15] prepared the mixture of SWNTs and DWNTs with a specific surface area of 790 m^2/g. The other common way, activation, is indirect. By activating CNTs using various activation agents, such as KOH [16, 17], CO_2, etc., the specific surface area of the activated CNTs can be increased because the ends of CNTs are opened and the walls of CNTs are etched, forming many micropores and mesopores. Raymundo-Pinero, et al. reported that MWNTs, prepared by catalytic decomposition of acetylene at 450, 500 and 600°C, when activated by KOH, showed porosity development during activation which had close related to the structural order of MWNTs [18]. MWNTs activated by various agents, such as KOH, CO_2 and air, might posses diverse pore structures, so there is a need to compare the activation effects and pore structures of such activated MWNTs.

In this paper, MWNTs prepared by the floating catalyst method at 1200°C were activated by KOH, CO_2 and air, and

Y. Chen · C. Liu · F. Li · H.-M. Cheng (✉)
Shenyang National Laboratory for Materials Science, Institute of Metal Research, Chinese Academy of Sciences, 72 Wenhua Road, Shenyang 110016, P.R. China
e-mail: cheng@imr.ac.cn

their pore structures were investigated. The morphologies of the activated MWNTs were examined by transmission electron microscopy (TEM) and the specific surface area and pore size distribution (PSD) of the activated MWNTs were analyzed by nitrogen adsorption measurements.

2. Experimental

The MWNTs with an average diameter about 30 nm used in our experiments were prepared by the floating catalyst method using benzene as the carbon source, hydrogen as the carrier gas, ferrocene as the catalyst precursor, and thiophene as the growth promoter [19].

2.1. Air and CO_2 activation processes

In order to remove amorphous carbon and catalyst metal contained in the as-prepared MWNTs, air oxidation and acid-washing were conducted. In detail, the pristine MWNT product was ultrasonicated in alcohol for 30 min to disperse the MWNTs and dried in air at 363 K. Then it was heated in a still air atmosphere at 673 K for 4 h. The material remaining after air oxidation was soaked in concentrated hydrochloric acid for 48 h and washed with deionized water until pH = 7. In order to completely eliminate catalyst and carbon impurities, the sample was again heated in air atmosphere at 713 K for 40 min, soaked in concentrated hydrochloric acid, washed with deionized water until pH = 7 and dried, The product of this procedure was called air-activated MWNTs. The activated MWNTs were treated at 1173 K for 1 h in argon atmosphere to remove adsorbed gases and oxygen containing functional groups. The treatment time was increased with the temperature decreasing, which led to part of the oxygen containing functional groups remained in the MWNTs according to the X-ray photoelectron spectrum (XPS) results and they blocked the micropores. The yield of air-activated MWNTs was about 40 wt.%.

Two CO_2-activated MWNTs were prepared as follows, and characterized in this study: CO_2-activated MWNTs-I: the as-prepared MWNTs were ultrasonicated in alcohol for 30 min and dried in air at 363 K, then treated at 1123 K for 4 h under flowing carbon dioxide, soaked in concentrated hydrochloric acid to remove the catalyst, and finally washed with the deionized water. CO_2-activated MWNTs-II: the air-activated MWNTs were treated at 1123 K for 4 h under the flowing carbon dioxide, soaked in concentrated hydrochloric acid to remove the catalyst, and then washed with the deionized water. Finally, both of the activated MWNTs were treated at 1173 K for 1 h in argon. About 36 wt.% of the CO_2-activated MWNTs-I and 45 wt.% of the CO_2-activated MWNTs-II remained.

2.2. KOH activation process

Ball milling of air-activated MWNTs and KOH powder was performed in a stainless steel vessel with stainless-steel balls in an inert gas atmosphere. The weight ratio of KOH to the MWNTs was 3:1. The milling time was 30 min, which resulted in a uniformly ground powder mixture. The mixture was then heated to 1123 K for 1 h under flowing argon in a horizontal tube furnace, washed in concentrated hydrochloric acid and the deionized water and dried. Finally, the activated MWNTs were treated at 1173 K for 1 h in argon. About 35 wt.% KOH-activated MWNTs were obtained.

2.3. Nitrogen adsorption measurements and structural analysis

The pore structures of the as-prepared and activated MWNTs were analyzed by liquid nitrogen adsorption measurements that were carried out by using a volumetric adsorption apparatus at 77.3 K. Before the measurements, all the MWNTs were outgassed in vacuum at 473 K and 10^{-4} Pa for 9 h. The specific surface area, pore volume and pore size distributions of all the MWNT samples were calculated from the measured adsorption isotherms.

3. Results and discussion

3.1. Morphologies of the activated MWNTs

From the TEM image shown in Fig. 1(a), it can be seen that there were amorphous carbon and catalyst particles remaining in the as-prepared MWNTs. After air-activation, most of the amorphous carbon and catalyst metals were removed and the MWNTs were opened or cut (Fig. 1(b)). The morphology of the CO_2-activated MWNTs-I (Fig. 1(c)) was similar to that of the air-activated MWNTs, but some MWNTs with a larger hollow cores than the as-prepared MWNTs were observed. This enlargement might have resulted from CO_2 oxidation of the inner wall of the MWNTs. The air and CO_2-activated MWNTs were long and straight, but after KOH activation, the MWNTs became much shorter due to the ball milling. Also their inner hollow cores had become enlarged, caused by KOH etching (Fig. 1(d)).

3.2. Adsorption isotherm analysis

Figure 2 shows the liquid N_2 adsorption isotherms of the different MWNTs. The KOH-activated MWNTs adsorbed much more nitrogen indicating a high specific surface area and high pore volume. An initial rapid increase in the nitrogen adsorbed by the activated MWNTs was observed

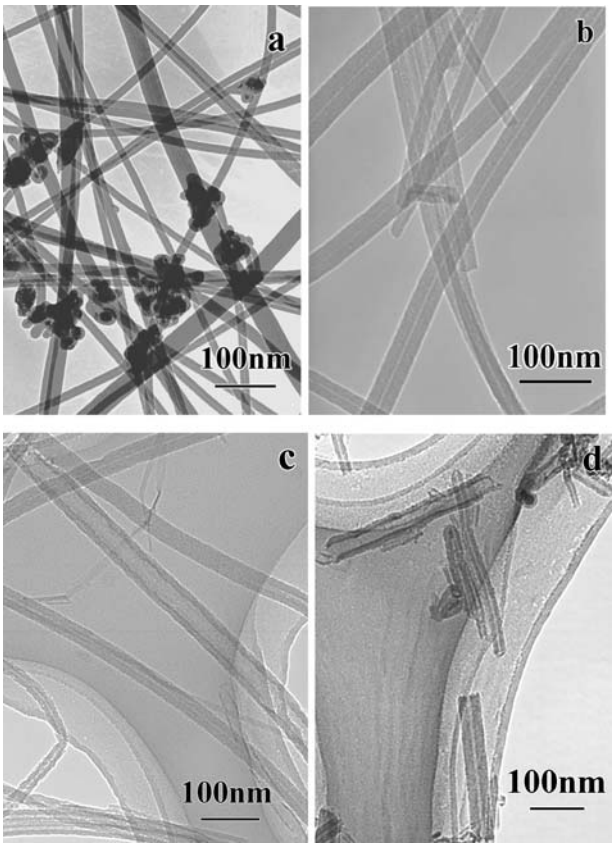

Fig. 1 TEM images of (a) the as-prepared MWNTs; (b) the air-activated MWNTs; (c) the CO_2-activated MWNTs; and (d) the KOH-activated MWNTs

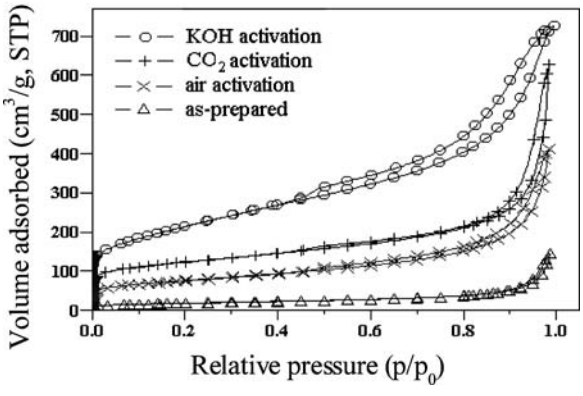

Fig. 2 The nitrogen adsorption isotherms of the as-prepared and activated MWNTs

below $P/P_0 = 0.05$, suggesting the presence of abundant micropores. On the other hand, a gradual uptake of N_2 was observed at the intermediate P/P_0, which indicated the adsorption of N_2 on the external surfaces of the activated MWNTs. The isotherms show that the external surface area of the KOH-activated material was greater than those of the CO_2 and air activated MWNTs. The isotherm of the CO_2-activated MWNTs-I overlapped or was very close to the CO_2-activated MWNTs-II, so only the isotherm of the CO_2-activated MWNTs-I was given. The marked appearance of hysteresis in the N_2isotherms in the high P/P_0 range indicates that activation had produced mesopores and opened the caps of the MWNTs. The isotherm of the as-prepared MWNT sample showed very little hysteresis. Among the activated MWNTs, the KOH activation process can produced the most mesopores.

The specific surface area and pore volume of the various MWNTs are shown in Table 1. The BET specific surface area of the as-prepared MWNTs was 65 m^2/g, while that of the air-activated sample was 270 m^2/g. According to the thermo-gravimetric analysis, the as-prepared MWNTs contained 10.2 wt.% metal catalyst, but here was only 1.0 wt.% in the purified MWNTs. So the increase of specific surface area by removal of the metal catalyst could have not made a magnificent contribution. Nevertheless, air oxidation was effective in removing amorphous carbon, opening the ends and creating micropores in the walls while increased the specific surface area and facilitated the access of the adsorbent (N_2) to the MWNT surfaces. The specific surface areas of the CO_2-activated MWNTs-I and -II were 429 m^2/g and 420 m^2/g, respectively, but the CO_2-activated MWNTs-I had a smaller mesopore volume than the CO_2-activated MWNTs-II. This difference was because of the further CO_2 activation having played a role in creating and enlarging the micropores. The highest specific surface area (785 m^2/g) was achieved by KOH-activation. The KOH-activated MWNTs also had the greatest pore volume, of both micropores and mesopores. The specific surface area of our KOH-activated MWNTs was smaller than that (about 868 m^2/g) reported by Raymundo-Pinero, because the as-prepared MWNTs we used were synthesized at a higher temperature (1200°C), while their MWNTs were prepared at 600°C [18]. Due to ball milling, our KOH-activated MWNTs were short cut to several hundred nanometers, instead of long nanotubes.

TEM and HRTEM observations revealed that many KOH-activated MWNTs had thin walls and the graphitic layers of these tubes (Fig. 3(a)) changed from two to three, and then four away from the open end tip due to etching. The

Table 1 The specific surface area and pore volume of MWNTs in different states

MWNTs	S_{BET} (m^2/g)	V_{mi} (cm^3/g)	V_{me} (cm^3/g)
As-prepared	65	0.01	0.12
Air-activated	270	0.06	0.56
CO_2-activated (I)	429	0.10	0.58
CO_2-activated (II)	420	0.10	0.67
KOH-activated	785	0.17	1.04

S_{BET}-BET specific surface area, V_{mi}-the micropore volume (diameter < 2 nm), V_{me} -the mesopore volume (2 nm <diameter < 50 nm).

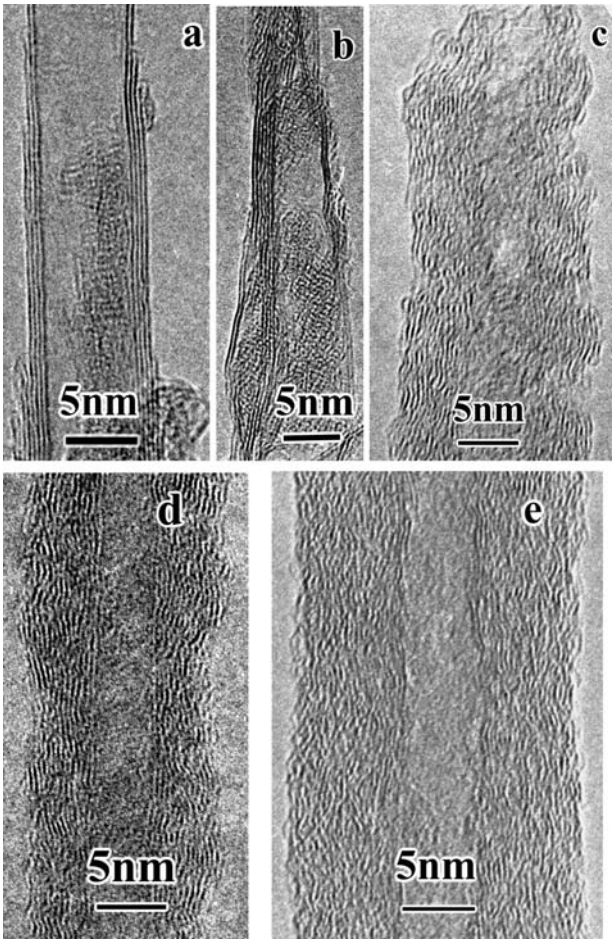

Fig. 3 HRTEM images of (a), (b) and (c) the KOH-activated MWNTs; (d) the CO_2-activated MWNTs; and (e) the air-activated MWNTs

specific surface area of MWNTs increases with the decrease of graphitic layers. Moreover, some graphitic layers in the KOH-activated MWNTs were separated to form a cuneiform pore (Fig. 3(b)), and some graphitic layers were removed to form an interlayer pore. From Fig. 3(c), it can be seen that the wall of some MWNTs was damaged creating many cavities. These factors can greatly increase the specific surface area and the micropore volume. Figure 3(d) and 3(e) show that the surface of the air-activated MWNTs was smoother than that of the CO_2-activated MWNTs, which caused the specific surface area and the micropore volume to be smaller than those of the CO_2-activated MWNTs.

3.3. Pore size distribution

The pore size distribution (PSD) is an important parameter for porous materials. In order to obtain micropore size distribution of the MWNTs, we used the Horvath-Kawazoe (HK) equation for a cylindrical pore model. In the mesopore region, the BJH equation is conventionally used to calculate the PSDs. Therefore, a combination of the HK (for < 2 nm region) and BJH (for 2–50 nm region) methods was used to obtain PSDs of the MWNTs from the adsorption branch of the isotherm, and the results are shown in Fig. 4. The PSDs of the KOH-activated MWNTs show two main peaks in the micropore region at 1.2 nm and 1.5 nm, respectively, and a peak in mesopore region at 2–4 nm. KOH not only can etch the carbon atoms on the tube walls to form micropores (Fig. 3(c)), but also can insert graphitic layers to form cuneiform (Fig. 3(b)) and interlayer pores. Some spherical onion-like pores were also found in the KOH-activated MWNTs because the high impact of the balls during ball milling could convert the local graphitic sheets of the tube walls at the impact points to onion-like particles. Similarly, it has been reported high impact of ball milling produced onion-like particles [20] and cup-stacked carbon nanotubes [21]. So the MWNTs activated by KOH were rich in micropores and mesopores. The PSDs of CO_2-activated MWNTs had two peaks at 1.2 nm and 1.5 nm in the micropore region and the PSD peak for the air-activated MWNTs was about 1.2 nm. Only the KOH-activated MWNTs had a PSD peak in the range of 2–5 nm in the mesopore region, suggesting that mesopores were produced by the etching of the walls and the inserting of graphitic layers. In the HRTEM images (Fig. 3), the interlayer pores (Fig. 3(b)) and etching pores (Fig. 3(b)) in the wall were in the range of 2–5 nm. Reaction of CO_2 or O_2 with carbon would have been from the surface inward, gradually with no intercalation or onion-like pores occurring. So, the MWNTs activated by CO_2 and air possess simpler pore structure distributions. The HRTEM images (Fig. 3(d) and 3(e)) revealed that the pores on the surface of the CO_2-activated MWNTs were deeper than those of the air-activated material, so the micropore volume of the CO_2-activated MWNTs was much higher than that of the air-activated sample. Since micropores did not exist in the as-prepared MWNTs, it was concluded that they were created in the activation processes.

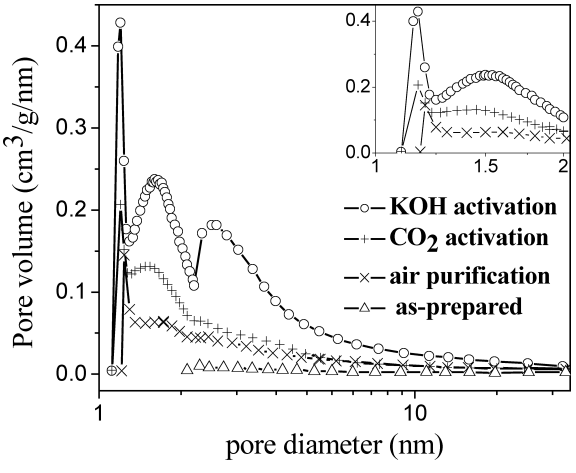

Fig. 4 Pore size distributions of the as-prepared and activated MWNTs

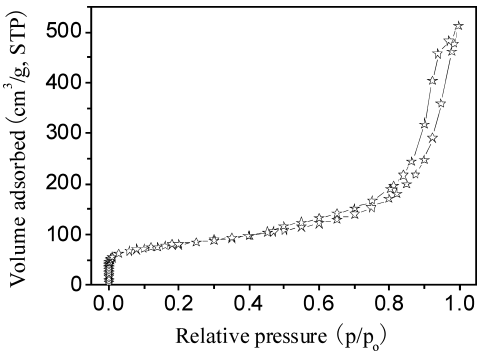

Fig. 5 The isotherm of the ball milled MWNTs

3.4. Activation mechanisms

Ball milling is a conventional and effective way to prepare some nanomaterials and to mix different components. During the ball milling process, the frequent collisions and high velocity of the steel balls cause major impacts on the material, which leads to cutting the MWNTs into short segments and opening of the inner hollow tubes [13, 14].

In order to separate out the effect of ball milling on the pore structure of MWNTs, Some air activated MWNTs were ball milled under the same conditions as the KOH activated MWNTs had been, but without the high temperature activation. Figure 5 shows the N_2 adsorption isotherm of this ball milled material. Compared to the air-activated MWNTs, the adsorption isotherm of the ball milled MWNTs showed a larger hysteresis loop. The specific surface area of the ball milled MWNTs was 283 m^2/g, 13 m^2/g more than that of the original air activated sample. The micropore and mesopore volumes were also increased to 0.06 and 0.76 cm^3/g from 0.06 and 0.56 cm^3/g, respectively. It was suggested that new pores were created during the ball milling process. From Fig. 6, we can see that the MWNTs were cut into short segments and some of these pieces were connected by a few inner graphitic layers which were not broken. Some MWNTs were even deformed into graphite sheets by the high impact of ball milling. Some new pores and defects were formed in the walls of the MWNTs during the ball milling process (Fig. 6(b)).

At the same time, the ball milling process uniformly disperses the KOH and MWNTs, which is very important for activation. During high temperature treatment, due to KOH etching, numerous micropores (Fig. 3(c)) were created on the external surface of the MWNTs, and some outer and inner graphitic layers were removed, so the nanotube walls became thinner (Fig. 3(a)). The potassium vapor can also enter the walls of the carbon nanotubes through all the outer and inner defects and expand the graphitic layers to form the interlayer pores. TEM and HRTEM observations revealed that some graphitic layers of the KOH-activated MWNTs were separated and even removed in some cases, which gave the evidence that K can be inserted insert into the graphitic layers.

The activation of MWNTs by CO_2 and air is a gas-solid reaction process, which is related with the reactivity and diffusion rate of gases. If the reaction is strong and rapid, the activator reacts with carbon on the external surface or on the wall of large pores before it diffuses into the micropores, so the pore depth will be short and the pore volume small. The reaction rate of carbon dioxide with carbon is far slower than that of the oxygen in air at high temperature. Therefore, during CO_2 activation the reaction rate can be balanced with the diffusion rate and more micropores can be formed. From TEM observations, it was found that some CO_2-activated MWNTs possessed larger hollow cores than the air-activated material. This result indicated that CO_2 can diffuse into the inner tube of MWNTs while O_2 does not. On the other hand, according to the reaction: $C + O_2(g) = CO_2(g)$, at 101325 Pa pressure

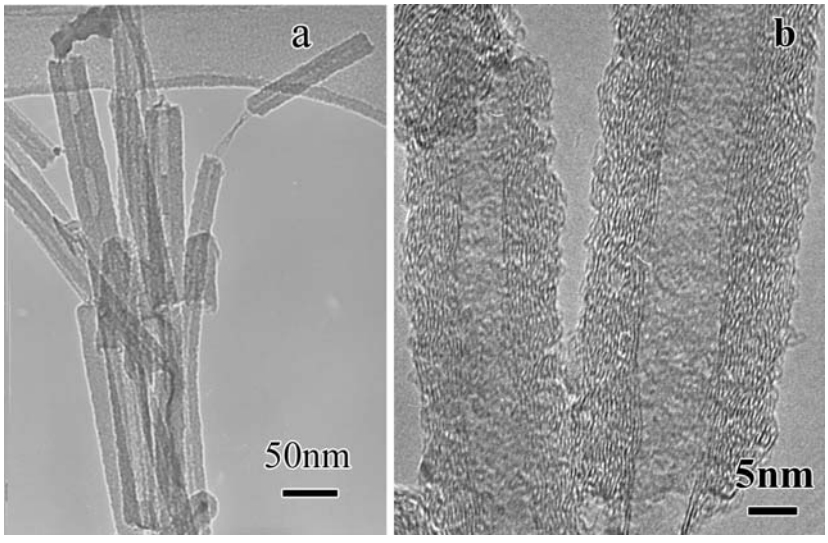

Fig. 6 TEM (a) and HRTEM (b) images of the ball milled MWNTs

and 713 K, the exothermic heat is −392.06 kJ/mol. The reaction of carbon with oxygen releases such a large quantity of heat that the local temperature may be greatly increased, which in turn promotes the reaction rate and causes the carbon of the MWNTs to be burned off. As a result, a large pore was formed. On the other hand, the reaction of carbon with carbon dioxide, $C + CO_2(g) = 2CO(g)$, is endothermic (at pressure of 101325 Pa and 1023 K, ΔH_f =169.63 kJ/mol). Therefore, the reactivity of carbon dioxide is much less than that of oxygen, and carbon dioxide can react more gently with the carbon, thus developing more micropores in the CO_2-activated sample.

4. Conclusions

Activation of MWNTs by air, CO_2 and KOH greatly increased their specific surface area and pore volumes. Ball-milling of the MWNTs with KOH followed by the high temperature treatment was the most effective activation method, and the KOH-activated material had more micropores and a higher specific surface area than the CO_2-activated and air-activated MWNTs. The PSD of the KOH-activated MWNTs showed two main peaks at 1.2 nm and 1.5 nm in the micropore region, and one peak in the mesopore region at 2–4 nm. KOH not only etched the graphitic layers to make the wall of the nanotubes thinner and formed micropores on the surface of MWNTs, but also intercalated into the graphitic layers to form cuneiform and interlayer pores. So, the MWNTs activated by KOH were rich in both micropores and mesopores. The PSD of the CO_2-activated MWNTs had two peaks at 1.2 nm and 1.5 nm in micropore region, while the PSD of the air-activated MWNTs possessed only one peak at 1.2 nm.

Acknowledgments We thank Prof. Max Lu of the University of Queensland, Australia for his valuable discussions. This work was supported by the Major State Basic Research Program (No. G2000026403) and Hi-Tech Research and Development Program (No. 2002AA302401) of MOST, China.

References

1. S. Iijima, Nature **354**, 56–8 (1991).
2. N. Pierard, A. Fonseca, Z. Konya, I. Willems, G.V. Tendeloo, and J.B. Nagy, Chem. Phys. Lett. **335**, 1 (2001).
3. M.L. Shofner, F.J. Rodríguez-Macías, R. Vaidyanathan, and E.V. Barrera,Composites **34**, 1207 (2003).
4. S.J. Wang, S.F. Yin, L. Li, B.Q. Xu, C.F. Ng, and C.T. Au, Appl. Catal. **52**, 287 (2004).
5. Z.B. He, J.H. Chen, D.Y. Liu, H. Tang, W. Deng, and Y.F. Kuang, Mater. Chem. Phys. **85**, 396 (2004).
6. N. Jonge and N.J. Druten, Ultramicroscopy **95**, 85 (2003).
7. G. Arabale, D. Wagh, M. Kulkarni, I.S. Mulla, S.P. Vernekar, and K. Vijayamohanan, et al. Chem. Phys. Lett. **376**, 207 (2003).
8. Q.F. Xiao and X. Zhou., Elec. Acta. **48**, 575 (2003).
9. M. Cinke, J. Li, W. Charles, J. Bauschlicher, A. Ricca, and M. Meyyappan, Chem. Phys. Lett. **376**, 761 (2003).
10. J.J. Zhao, A. Buldum, J. Han, and J.P. Lu, Nanotechnol. **13**, 195 (2002).
11. A. Peigney, C. Laurent, E. Flahaut, R.R. Bacsa, and A. Rousset, Carbon **39**, 507 (2001).
12. K.L. Lu, R.M. Lago, Y.K. Chen, M.L. Green, P.J. Harris, and S.C. Tsang, Carbon **34**, 814 (1996).
13. K. Awasthi, R. Kamalakaran, A.K. Singh, and O.N. Srivastava, Int. J. Hydrogen Energy **27**, 425–32 (2002).
14. F. Liu, X.B. Zhang, J.P. Cheng, J.P. Tu, F.Z. Kong, W.Z. Huang, et al. Carbon **41**, 2527 (2003).
15. R.R. Bacsa, C. Laurent, A. Peigney, W.S. Bacsa, T. Vaugien, and A. Rousset, Chem. Phys. Lett. **323**, 566 (2000).
16. Q. Jiang, M.Z. Qu, B.L. Zhang, and Z.L. Yu , Carbon **40**, 2743 (2002).
17. E. Raymundo-Pinero, D. Cazorla-Amoros, A. Linares-Solano, S. Delpeux, E. Frackowiak, K. Szostak, et al. Carbon **40**, 1614 (2002).
18. E. Raymundo-Pinero, P. Azais, T. Cacciaguerra, D. Cazorla-Amoros, A. Linares-Solano, and F. Beguin, Carbon **43**, 786 (2005).
19. Y.Y. Fan, F. Li, H.M. Cheng, G. Su, Y.D. Yu, and Z.H. Shen, J. Mater. Res. **13**, 2342 (1998).
20. Y.B. Li, B.Q. Wei, J. Liang, Q. Yu, and D.H. Wu, Carbon **37**, 493 (1999).
21. Y.A. Kim, T. Hayashi, Y. Fukai, M. Endo, T. Yanagisawa, and M.S. Dresselhaus, Chem. Phys. Lett. **355**, 279 (2002).